

Pure Molecular Beam of Water Dimer

Helen Bieker,^{1, 2, 3} Jolijn Onvlee,¹ Melby Johny,^{1, 2} Lanhai He,^{1, ||} Thomas Kierspel,^{1, 2, 3, §}
Sebastian Trippel,^{1, 3} Daniel A. Horke,^{1, 3, ‡} and Jochen Küpper^{1, 2, 3, *}

¹Center for Free-Electron Laser Science, Deutsches Elektronen-Synchrotron DESY, Notkestraße 85, 22607 Hamburg, Germany

²Department of Physics, Universität Hamburg, Luruper Chaussee 149, 22761 Hamburg, Germany

³Center for Ultrafast Imaging, Universität Hamburg, Luruper Chaussee 149, 22761 Hamburg, Germany

Spatial separation of water dimer from water monomer and larger water-clusters through the electric deflector is presented. A beam of water dimer with 93 % purity and a rotational temperature of 1.5 K was obtained. Following strong-field ionization using a 35 fs laser pulse with a wavelength centered around 800 nm and a peak intensity of 10^{14} W/cm² we observed proton transfer and 46 % of the ionized water dimer broke apart into a hydronium ion H₃O⁺ and OH.

Hydrogen bonding between water molecules plays an important role in aqueous systems, e. g., for biomolecules that are surrounded by solvents. It is responsible for the unique properties of water, such as its high boiling point [1]. While hydrogen bonds have been studied extensively in many different molecular systems [2–8], one of the most important models remains the water dimer, somehow the smallest drop of water. Numerous studies have been conducted on this benchmark system and its structure with a single hydrogen bond is well known [9–12].

Water and water-clusters have been studied using various techniques to describe dynamics such as proton motion [13] or chemical processes, e. g., reactive collisions [14]. For investigations of ultrafast molecular dynamics, such as energy and charge transfer across hydrogen bonds in molecular systems, photoion-photoion coincidence measurements at free-electron lasers are developing as a powerful tool [8, 15, 16] and this approach was also used to study hydrogen bonding in the water dimer at a synchrotron [17]. Other spectroscopic techniques utilizing synchrotron facilities [18, 19] or table-top laser-systems [5, 6, 20, 21] further improved the knowledge about hydrogen bonding in water and water-clusters.

Most of these experiments investigating the dynamics of hydrogen-bonded systems would benefit from samples of identical molecules in a well-defined initial state. The widely used supersonic expansion technique provides cold molecular beams down to rotational temperatures of < 1 K [22–24]. However, cluster expansions do not produce single-species beams, but a mixture of various cluster stoichiometries. Hence, only a low concentrations of specific species can be achieved. In the case of water, supersonic expansion produces a cold beam of various water clusters [2] with a water dimer concentration of only a few percent [17, 25]. This leads to small experimental event rates and requires long measurement times, e. g., in coincidence detection schemes [16, 17]. These experiments with a mixture of molecules in a molecular beam are only feasible if it can be disentangled which molecule was actually measured. Therefore, these mixtures severely limit the applicable techniques. A pure

beam of water dimer would significantly speed up the measurements, when unwanted backgrounds from carrier gas and larger water-clusters are avoided, or simply enable such experiments.

The electrostatic deflector is an established method to spatially separate the molecules of interest from the carrier gas and to separate different species within a cold molecular beam [26]. This includes the separation of molecular conformers [27–30], individual quantum states of small molecules [31, 32], as well as specific molecular clusters [24, 33, 34]. The deflector was previously utilized in investigations of water, e. g., to determine the rotational temperatures of “warm” molecular beams of water [35], to separate its *para* and *ortho* species [32], and to measure the dipole moment of small water-clusters [36]. Spatially separated single-species samples enable, for instance, advanced imaging applications of water-clusters using non-species-specific techniques, as well as the study of size-specific effects and the transition from single-molecule to bulk behavior.

Here, the electrostatic deflector was used to spatially separate water dimer from water and larger water-clusters in a molecular beam formed by supersonic expansion. The experimental setup was described previously [26, 37]. Briefly, liquid water was placed in the reservoir of an Even-Lavie valve [23], heated to 55 °C, seeded in 100 bar of helium, and expanded into vacuum with a nominal driving-pulse duration of 19.5 µs and at a repetition rate of 250 Hz. The produced molecular beam was doubly skimmed, 6.5 cm ($\varnothing = 3$ mm) and 30.2 cm ($\varnothing = 1.5$ mm) downstream from the nozzle, directed through the electrostatic deflector [38] of 154 mm length and with a nominal field strength of 50 kV/cm with an applied voltage of 8 kV across the deflector, before passing through a third skimmer ($\varnothing = 1.5$ mm). The deflector was placed 4.4 cm behind the tip of the second skimmer. In the center of a time-of-flight (TOF) mass spectrometer, 134.5 cm downstream from the nozzle, molecules were strong-field ionized by a 35 fs short laser pulse with a central wavelength around 800 nm and a pulse energy of 170 µJ. Focusing to 65 µm yielded a peak intensity of $\sim 10^{14}$ W/cm². The generated ions were accelerated toward a microchannel-

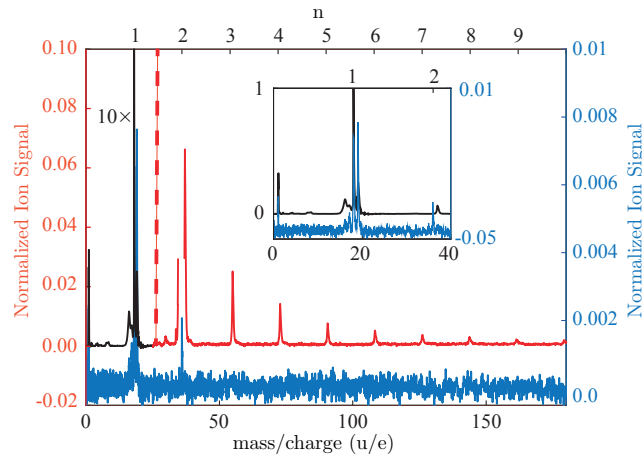


FIG. 1. TOF-MS in the center of the molecular beam as depicted in Fig. 2 with a deflector voltage of 0 kV (black, red) and at a position of +3 mm with a deflector voltage of 8 kV (blue). For mass/charge (m/q) ratios of 0...30 u/e, to the left of the dashed red line, the TOF-MS has been scaled by 0.1. The inset shows the region of m/q = 0...40 u/e enlarged; see text for details.

plate detector combined with a phosphor screen and the generated signal was recorded with a digitizer. The valve, skimmers, and deflector were placed on motorized translation stages, which allowed movement of the molecular beam through the ionization laser focus and the recording of vertical molecular-beam-density profiles without moving the laser focus, resulting in fixed imaging conditions [39–41].

While the employed strong-field ionization is a general, non-species specific ionization technique, it can also lead to fragmentation of molecules, such that recorded mass spectra (MS) do not directly reflect the composition of the molecular beam. In combination with the species-specific deflection process, however, this can be disentangled and, thus, even allows for the investigation of strong-field-induced fragmentation processes of a single species.

TOF-MS of the direct and the deflected beams are shown in Fig. 1. The spectrum of the undeflected beam shows water-cluster ions $(\text{H}_2\text{O})_n^+$ up to $n = 2$ and protonated water-cluster ions $(\text{H}_2\text{O})_n\text{H}^+$ up to $n = 10$. Even larger clusters were likely formed in the supersonic expansion, but were not observed in the recorded TOF interval. We point out that all clusters that reach the interaction region are neutral clusters of the type $(\text{H}_2\text{O})_n$, and protonated clusters must result from the interactions with the femtosecond laser, i.e., due to fragmentation during or after the strong-field-ionization process.

Vertical molecular-beam-density profiles for water ions $(\text{H}_2\text{O})^+$, water dimer ions $(\text{H}_2\text{O})_2^+$, and protonated water-cluster ions $(\text{H}_2\text{O})_n\text{H}^+$ up to $n = 4$, with a potential difference of 8 kV applied across the deflector, are shown in Fig. 2. For comparison, a field-free vertical profile for

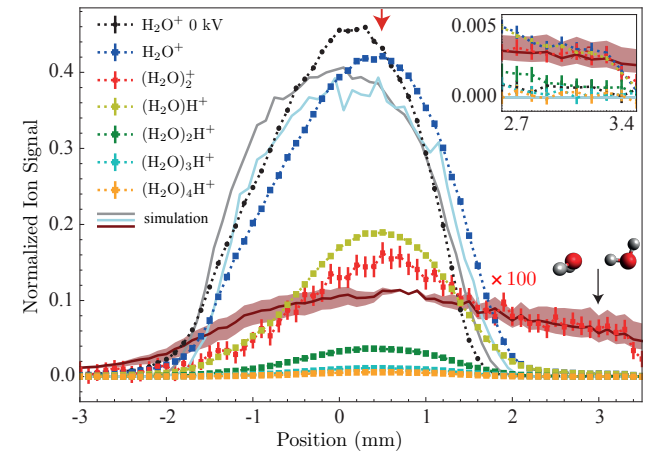


FIG. 2. Normalized measured vertical molecular-beam-density profiles (dashed lines) of water $(\text{H}_2\text{O})^+$ (blue), water dimer $(\text{H}_2\text{O})_2^+$ (red) and protonated water-cluster ions $(\text{H}_2\text{O})_n\text{H}^+$ up to $n = 4$ (yellow, green, cyan, orange) with deflector voltages of 0 kV (black circles) and 8 kV (squares). Simulated vertical molecular-beam-density profiles of water at a deflector voltage of 0 kV (grey) as well as of water (light blue) and water dimer (dark red) with a deflector voltage of 8 kV are shown as solid lines. The shaded darkred area is the error of the water dimer simulation in the temperature range of $T_{\text{rot}} = 1.5(5)$ K; see text for details. The black arrow indicates the position in the deflected beam where the TOF of Fig. 1 has been measured. The inset shows the deflection region enlarged with a magnification factor of 5 applied to the $(\text{H}_2\text{O})_2^+$ and $(\text{H}_2\text{O})_n\text{H}^+$ signals.

the water ion with 0 kV across the deflector is also shown. The vertical molecular-beam-density profiles have been normalized to the area of the field-free spatial profile of the water ion. For visibility the water dimer profile has been scaled by a factor of 100 after normalization. While the field-free molecular beam profile is centered around 0 mm, application of a voltage of 8 kV to the deflector shifted the peak of water ions, water dimer ions, and protonated water-cluster ions by +0.5 mm, as indicated by the red arrow in Fig. 2. In addition, the water-dimer ion showed a broadening and an increase of signal at around +3 mm, indicated by a black arrow in Fig. 2.

In the inset of Fig. 2 the region around +3 mm is shown enlarged with a magnification factor of 5 applied to $(\text{H}_2\text{O})_2^+$ and $(\text{H}_2\text{O})_n\text{H}^+$ with $n = 1\dots 4$. The corresponding TOF-MS in the deflected part of the beam at a position of +3 mm is highlighted in Fig. 1 by the blue line. Not just the water dimer ion, but also the hydronium ion H_3O^+ and the water ion showed an increased signal in the deflected beam. The shape of the vertical beam profiles for these ions matched the water dimer profile in the region of 2.8–3.5 mm, indicating that they originated from the same parent molecule.

The water dimer ion was the largest non-protonated cluster measured in this setup. To verify that the water

dimer ion was originating from the water dimer, the deflection behaviour of water-clusters inside the electrostatic deflector was simulated. Therefore, the Stark energies and effective dipole moments of water and water-clusters were calculated with the freely available CMISTARK software package [42] using rotational constants, dipole moments, and centrifugal distortion constants from the literature [11, 43–46], see Suppl. Inf. Table I; contributions of the polarizability to the Stark effect could safely be ignored [38, 47]. The effective dipole moment for water dimer is much larger than for water, leading to a larger acceleration in the electric field in the deflector, see Fig. 3 of the Suppl. Inf. for further information.

The simulated vertical molecular-beam-density profiles of water and water dimer are shown in Fig. 2. Due to the rotational-state dependence of the Stark effect, the deflection of a molecular beam in an electrostatic field depends on the rotational temperature of the molecular ensemble [26] and the best fit was obtained assuming a Maxwell-Boltzmann population distribution of rotational states corresponding to 1.5(5) K.

Not only deflection of water dimer, but also of all protonated-cluster ions has been measured, for instance, for $(\text{H}_2\text{O})_2^+$, as indicated by the red arrow and symbols in Fig. 2. Trajectory simulations for water-clusters $(\text{H}_2\text{O})_n^+$ with $n = 3 \dots 7$ were performed to understand the origin of this deflection behavior. These showed that, based on the different effective dipole moments, a different deflection is expected for different water-clusters, see Fig. 5 of the Suppl. Inf.. Since the detected protonated water-clusters arose from the strong-field fragmentation of larger neutral clusters in the interaction region, the measured vertical protonated-cluster density profiles are a superposition of several neutral water-cluster density profiles. Thus, it is not possible to compare the individual simulated molecular-beam-density profiles of neutral clusters directly with the measured protonated water-cluster density profiles. Instead, at each position of the deflection profile the signal from all water-clusters has been summed up, both for the simulated and the measured molecular-beam-density profiles. The result yields a comparable amount of deflection for simulated and measured molecular-beam-density profiles, see Suppl. Inf. Fig. 6. The shift of 0.5 mm can, therefore, originate from the superimposed molecular-beam-density profiles from different larger clusters due to fragmentation into smaller water-clusters. The same shift is visible for H_2O^+ and $(\text{H}_2\text{O})_2^+$, which indicates that water-clusters are also fragmenting into H_2O^+ and $(\text{H}_2\text{O})_2^+$. Nevertheless, the simulation for water-clusters $n = 1 \dots 7$ shows that water dimer deflected the most, reaching a position of +3 mm and above, see Suppl. Inf. Fig. 4 and Fig. 5. Of all the other clusters considered, only the water hexamer in its prism and book forms reaches to a position up to 3.2 mm with the falling edge of the profile. The water hexamer has only been measured as a fragment and the amount of water hexamer

in the molecular beam is unknown. Assuming an exponential water-cluster distribution, the amount of water hexamer in the deflected molecular beam is negligibly small.

The TOF-MS in the deflected part of the beam, shown in Fig. 1, contains peaks corresponding to H^+ , O^+ , OH^+ , H_2O^+ , and H_3O^+ , in addition to the water-dimer ion. As mentioned before the short-pulse ionization can lead to fragmentation. For water dimer, two fragmentation channels were reported for electron-impact ionization with 70 eV electrons [48]: either an H_3O^+ ion and a neutral OH are formed or a H_2O^+ ion and a neutral water monomer H_2O . Comparison of the vertical molecular-beam-density profiles of the deflected molecules allowed further investigation of the fragmentation channels of the water dimer. The measured vertical molecular-beam-density profiles of these molecules showed a similar deflection behavior in the region of 2.8 to 3.5 mm as the water dimer, see Fig. 2 and Suppl. Inf. Fig. 1. The observed constant ratio of those fragments over this spatial region indicates that all these fragments originated from water dimer.

Comparing the intensity of the fragments of water dimer, H_2O^+ and H_3O^+ and $(\text{H}_2\text{O})_2^+$, in the deflected beam, the fragmentation ratios of the intact water dimer were estimated. These showed that 46(7) % of water dimer fragmented into one ionized water molecule, while 46(4) % of water dimer underwent most likely proton transfer and formed a hydronium ion. Only 8(2) % of the water dimer present in the molecular beam stayed intact after ionization.

The actual number of water-dimer molecules per shot in the deflected molecular beam was estimated to ~ 0.8 within the laser focus using the known fragmentation ratios of H_2O^+ and H_3O^+ into account, while the fragmentation channels of H^+ , O^+ , OH^+ have not been included. Taking the known fragmentation channels into account, the fraction of water dimer within the molecular beam was evaluated. Comparing the ratios between water dimer and all other species visible in the TOF, a water dimer fraction of 3.9(6) % in the center of the undeflected beam and of 93(15) % in the deflected beam, at a position of +3 mm, was achieved. Thus, using the electrostatic deflector the fraction of water dimer within the interaction region could be increased by nearly a factor of 24.

In summary, a high-purity beam of water dimer was created using the electrostatic deflector, which spatially separated water dimer from other species present in the molecular beam. The resulting water dimer sample had a purity of 93(15) %. The fragmentation products and ratios of water dimer following strong-field ionization using a 35 fs laser pulse with a wavelength centered around 800 nm and peak intensity of $\sim 10^{14} \text{ W/cm}^2$ were studied, with 46(4) % of water dimer found to form hydronium ions and 46(7) % fragmenting into one water cation and one neutral water, while 8(2) % of water dimer stayed intact. The deflection profiles could be simulated using a rigid-rotor

model and an initial rotational temperature of 1.5(5) K.

The produced clean samples of water dimer are well suited for non-species-specific experiments, e.g., reactive-collisions, diffractive imaging, or ultrafast spectroscopies [14, 39, 49]. Even for experiments that can distinguish different species, for example photoion-photoion coincidence measurements [8, 50], the produced clean beams will enable significantly faster measurements of this important hydrogen-bonded model system, e.g., because unwanted backgrounds are avoided. Furthermore, the electrostatic separation technique can be used to separate different conformers [26], which could be highly interesting in the purification and studies of larger water-clusters that exhibit multiple conformers [51].

ACKNOWLEDGMENTS

This work has been supported by the Clusters of Excellence “Center for Ultrafast Imaging” (CUI, EXC 1074, ID 194651731) and “Advanced Imaging of Matter” (AIM, EXC 2056, ID 390715994) of the Deutsche Forschungsgemeinschaft (DFG), by the European Union’s Horizon 2020 research and innovation program under the Marie Skłodowska-Curie Grant Agreement 641789 “Molecular Electron Dynamics investigated by Intense Fields and Attosecond Pulses” (MEDEA), by the European Research Council under the European Union’s Seventh Framework Program (FP7/2007-2013) through the Consolidator Grant COMOTION (ERC-Küpper-614507), and by the Helmholtz Gemeinschaft through the “Impuls- und Vernetzungsfond”. L.H. acknowledges a fellowship within the framework of the Helmholtz-OCPC postdoctoral exchange program and J.O. gratefully acknowledges a fellowship by the Alexander von Humboldt Foundation.

and microsolvation of DF after F-atom reactions in polar solvents,” *Science* **347**, 530–533 (2015).

- [5] G. Berden, W. L. Meerts, M. Schmitt, and K. Kleinermanns, “High resolution UV spectroscopy of phenol and the hydrogen bonded phenol-water cluster,” *J. Chem. Phys.* **104**, 972 (1996).
- [6] T. M. Korter, D. W. Pratt, and J. Küpper, “Indole-H₂O in the gas phase. Structures, barriers to internal motion, and S₁ ← S₀ transition moment orientation. Solvent reorganization in the electronically excited state,” *J. Phys. Chem. A* **102**, 7211–7216 (1998).
- [7] A. L. Sobolewski and W. Domcke, “Photoinduced electron and proton transfer in phenol and its clusters with water and ammonia,” *J. Phys. Chem. A* **105**, 9275–9283 (2001).
- [8] X. Ren, E. Wang, A. D. Skitnevskaya, A. B. Trofimov, G. Kirill, and A. Dorn, “Experimental evidence for ultrafast intermolecular relaxation processes in hydrated biomolecules,” *Nat. Phys.* **79**, 1745 (2018).
- [9] J. A. Odutola and T. R. Dyke, “Partially deuterated water dimers: Microwave spectra and structure,” *J. Chem. Phys.* **72**, 5062–5070 (1980).
- [10] H. Yu and W. F. van Gunsteren, “Charge-on-spring polarizable water models revisited: From water clusters to liquid water to ice,” *J. Chem. Phys.* **121**, 9549–9564 (2004).
- [11] T. R. Dyke, K. M. Mack, and J. S. Muenter, “The structure of water dimer from molecular beam electric resonance spectroscopy,” *J. Chem. Phys.* **66**, 498–510 (1977).
- [12] T. R. Dyke and J. S. Muenter, “Molecular-beam electric deflection studies of water polymers,” *J. Chem. Phys.* **57**, 5011 (1972).
- [13] T. Marchenko, L. Inhester, G. Goldsztejn, O. Travnikova, L. Journel, R. Guillemin, I. Ismail, D. Koulentianos, D. Céolin, R. Püttner, M. N. Piancastelli, and M. Simon, “Ultrafast nuclear dynamics in the doubly-core-ionized water molecule observed via auger spectroscopy,” *Phys. Rev. A* **98**, 063403 (2018).
- [14] A. Kilaj, H. Gao, D. Rösch, U. Rivero, J. Küpper, and S. Willitsch, “Observation of different reactivities of para- and ortho-water towards trapped diazenylium ions,” *Nat. Commun.* **9**, 2096 (2018).
- [15] R. Boll, B. Erk, R. Coffee, S. Trippel, T. Kierspel, C. Bomme, J. D. Bozek, M. Burkett, S. Carron, K. R. Ferguson, L. Foucar, J. Küpper, T. Marchenko, C. Miron, M. Patanen, T. Osipov, S. Schorb, M. Simon, M. Swiggers, S. Techert, K. Ueda, C. Bostedt, D. Rolles, and A. Rudenko, “Charge transfer in dissociating iodomethane and fluoromethane molecules ionized by intense femtosecond x-ray pulses,” *Struct. Dyn.* **3**, 043207 (2016).
- [16] T. Kierspel, *Imaging structure and dynamics using controlled molecules*, Dissertation, Universität Hamburg, Hamburg, Germany (2016).
- [17] T. Jahnke, H. Sann, T. Havermeier, K. Kreidi, C. Stuck, M. Meckel, M. Schöffler, N. Neumann, R. Wallauer, S. Voss, A. Czasch, O. Jagutzki, A. Malakzadeh, F. Afaneh, T. Weber, H. Schmidt-Böcking, and R. Dörner, “Ultrafast energy transfer between water molecules,” *Nat. Phys.* **6**, 139–142 (2010).
- [18] B. Winter, E. F. Aziz, U. Hergenhahn, M. Faubel, and I. V. Hertel, “Hydrogen bonds in liquid water studied by photoelectron spectroscopy,” *J. Chem. Phys.* **126**, 124504 (2007).

|| Permanent address: Institute of Atomic and Molecular Physics, Jilin University, Changchun 130012, China

§ Present address: Department of Chemistry, University of Basel, Klingelbergstrasse 80, 4056 Basel, Switzerland

† Present address: Institute for Molecules and Materials, Radboud University, Heijendaalseweg 135, 6525 AJ Nijmegen, The Netherlands

* Corresponding author: jochen.kuepper@cfel.de; <https://www.controlled-molecule-imaging.org>

- [1] G. A. Jeffrey, *An Introduction to Hydrogen Bonding* (Oxford University Press, 1997).
- [2] K. Liu, J. Cruzan, and R. Saykally, “Water clusters,” *Science* **271**, 929–933 (1996).
- [3] K. Nauta and R. E. Miller, “Formation of cyclic water hexamer in liquid helium: The smallest piece of ice,” *Science* **287**, 293 (2000).
- [4] G. T. Dunning, D. R. Glowacki, T. J. Preston, S. J. Greaves, G. M. Greetham, I. P. Clark, M. Towrie, J. N. Harvey, and A. J. Orr-Ewing, “Vibrational relaxation

- [19] J. D. Smith, C. D. Cappa, K. R. Wilson, B. M. Messer, R. C. Cohen, and R. J. Saykally, “Energetics of hydrogen bond network rearrangements in liquid water,” *Science* **306**, 851–853 (2004).
- [20] F. N. Keutsch and R. J. Saykally, “Inaugural article: Water clusters: Untangling the mysteries of the liquid, one molecule at a time,” *PNAS* **98**, 10533–10540 (2001).
- [21] T. S. Zwier, “The spectroscopy of solvation in hydrogen-bonded aromatic clusters,” *Annu. Rev. Phys. Chem.* **47**, 205–241 (1996).
- [22] G. Scoles, ed., *Atomic and molecular beam methods*, Vol. 1 (Oxford University Press, New York, NY, USA, 1988).
- [23] U. Even, J. Jortner, D. Noy, N. Lavie, and N. Cossart-Magos, “Cooling of large molecules below 1 K and He clusters formation,” *J. Chem. Phys.* **112**, 8068–8071 (2000).
- [24] M. Johny, J. Onvlee, T. Kierspel, H. Bieker, S. Trippel, and J. Küpper, “Spatial separation of pyrrole and pyrrole-water clusters,” *Chem. Phys. Lett.* **721**, 149–152 (2019), arXiv:1901.05267 [physics].
- [25] J. B. Paul, C. P. Collier, R. J. Saykally, J. J. Scherer, and A. O’Keefe, “Direct measurement of water cluster concentrations by infrared cavity ringdown laser absorption spectroscopy,” *J. Phys. Chem. A* **101**, 5211–5214 (1997).
- [26] Y.-P. Chang, D. A. Horke, S. Trippel, and J. Küpper, “Spatially-controlled complex molecules and their applications,” *Int. Rev. Phys. Chem.* **34**, 557–590 (2015), arXiv:1505.05632 [physics].
- [27] F. Filsinger, U. Erlekam, G. von Helden, J. Küpper, and G. Meijer, “Selector for structural isomers of neutral molecules,” *Phys. Rev. Lett.* **100**, 133003 (2008), arXiv:0802.2795 [physics].
- [28] F. Filsinger, J. Küpper, G. Meijer, J. L. Hansen, J. Maurer, J. H. Nielsen, L. Holmegaard, and H. Stapelfeldt, “Pure samples of individual conformers: the separation of stereo-isomers of complex molecules using electric fields,” *Angew. Chem. Int. Ed.* **48**, 6900–6902 (2009).
- [29] T. Kierspel, D. A. Horke, Y.-P. Chang, and J. Küpper, “Spatially separated polar samples of the *cis* and *trans* conformers of 3-fluorophenol,” *Chem. Phys. Lett.* **591**, 130–132 (2014), arXiv:1312.4417 [physics].
- [30] N. Teschmit, D. A. Horke, and J. Küpper, “Spatially separating the conformers of the dipeptide Ac-Phe-Cys-NH₂,” *Angew. Chem. Int. Ed.* **57**, 13775–13779 (2018), arXiv:1805.12396 [physics].
- [31] J. H. Nielsen, P. Simesen, C. Z. Bisgaard, H. Stapelfeldt, F. Filsinger, B. Friedrich, G. Meijer, and J. Küpper, “Stark-selected beam of ground-state OCS molecules characterized by revivals of impulsive alignment,” *Phys. Chem. Chem. Phys.* **13**, 18971–18975 (2011), arXiv:1105.2413 [physics].
- [32] D. A. Horke, Y.-P. Chang, K. Dlugolecki, and J. Küpper, “Separating para and ortho water,” *Angew. Chem. Int. Ed.* **53**, 11965–11968 (2014), arXiv:1407.2056 [physics].
- [33] S. Trippel, Y.-P. Chang, S. Stern, T. Mullins, L. Holmegaard, and J. Küpper, “Spatial separation of state- and size-selected neutral clusters,” *Phys. Rev. A* **86**, 033202 (2012), arXiv:1208.4935 [physics].
- [34] H. S. You, J. Kim, S. Han, D.-S. Ahn, J. S. Lim, and S. K. Kim, “Spatial isolation of conformational isomers of hydroquinone and its water cluster using the stark deflector,” *J. Phys. Chem. A* **122**, 1194 (2018).
- [35] R. Moro, J. Bulthuis, J. Heinrich, and V. V. Kresin, “Electrostatic deflection of the water molecule: A fundamental asymmetric rotor,” *Phys. Rev. A* **75**, 013415 (2007).
- [36] R. Moro, R. Rabinovitch, C. Xia, and V. V. Kresin, “Electric dipole moments of water clusters from a beam deflection measurement,” *Phys. Rev. Lett.* **97**, 123401 (2006).
- [37] S. Trippel, M. Johny, T. Kierspel, J. Onvlee, H. Bieker, H. Ye, T. Mullins, L. Gumprecht, K. Dlugolecki, and J. Küpper, “Knife edge skimming for improved separation of molecular species by the deflector,” *Rev. Sci. Instrum.* **89**, 096110 (2018), arXiv:1802.04053 [physics].
- [38] J. S. Kienitz, K. Dlugolecki, S. Trippel, and J. Küpper, “Improved spatial separation of neutral molecules,” *J. Chem. Phys.* **147**, 024304 (2017), arXiv:1704.08912 [physics].
- [39] J. Küpper, S. Stern, L. Holmegaard, F. Filsinger, A. Rouzée, A. Rudenko, P. Johnsson, A. V. Martin, M. Adolph, A. Aquila, S. Bajt, A. Barty, C. Bostedt, J. Bozek, C. Caleman, R. Coffee, N. Coppola, T. Delmas, S. Epp, B. Erk, L. Foucar, T. Gorkhov, L. Gumprecht, A. Hartmann, R. Hartmann, G. Hauser, P. Holl, A. Hönke, N. Kimmel, F. Krasniqi, K.-U. Kühnel, J. Maurer, M. Messerschmidt, R. Moshammer, C. Reich, B. Rudek, R. Santra, I. Schlichting, C. Schmidt, S. Schorb, J. Schulz, H. Soltau, J. C. H. Spence, D. Starodub, L. Strüder, J. Thøgersen, M. J. J. Vrakking, G. Weidenspointner, T. A. White, C. Wunderer, G. Meijer, J. Ullrich, H. Stapelfeldt, D. Rolles, and H. N. Chapman, “X-ray diffraction from isolated and strongly aligned gas-phase molecules with a free-electron laser,” *Phys. Rev. Lett.* **112**, 083002 (2014), arXiv:1307.4577 [physics].
- [40] S. Stern, L. Holmegaard, F. Filsinger, A. Rouzée, A. Rudenko, P. Johnsson, A. V. Martin, A. Barty, C. Bostedt, J. D. Bozek, R. N. Coffee, S. Epp, B. Erk, L. Foucar, R. Hartmann, N. Kimmel, K.-U. Kühnel, J. Maurer, M. Messerschmidt, B. Rudek, D. G. Starodub, J. Thøgersen, G. Weidenspointner, T. A. White, H. Stapelfeldt, D. Rolles, H. N. Chapman, and J. Küpper, “Toward atomic resolution diffractive imaging of isolated molecules with x-ray free-electron lasers,” *Faraday Disc.* **171**, 393 (2014), arXiv:1403.2553 [physics].
- [41] F. Filsinger, J. Küpper, G. Meijer, L. Holmegaard, J. H. Nielsen, I. Nevo, J. L. Hansen, and H. Stapelfeldt, “Quantum-state selection, alignment, and orientation of large molecules using static electric and laser fields,” *J. Chem. Phys.* **131**, 064309 (2009), arXiv:0903.5413 [physics].
- [42] Y.-P. Chang, F. Filsinger, B. Sartakov, and J. Küpper, “CMISTARK: Python package for the stark-effect calculation and symmetry classification of linear, symmetric and asymmetric top wavefunctions in dc electric fields,” *Comp. Phys. Comm.* **185**, 339–349 (2014), arXiv:1308.4076 [physics].
- [43] F. C. DeLucia, P. Helminger, and W. H. Kirchhoff, “Microwave spectra of molecules of astrophysical interest V. Water vapor,” *J. Phys. Chem. Ref. Data* **3**, 211–219 (1974).
- [44] L. H. Coudert and J. T. Hougen, “Analysis of the microwave and far infrared spectrum of the water dimer,” *Journal Of Molecular Spectroscopy* **139**, 259–277 (1990).
- [45] S. L. Shostak, W. L. Ebenstein, and J. S. Muenter, “The dipole moment of water. I. dipole moments and hyperfine properties of H₂O and HDO in the ground and excited vibrational states,” *J. Chem. Phys.* **94**, 5875 (1991).
- [46] N. P. Malomuzh, V. N. Makhlaichuk, and S. V. Khrapatyi, “Water dimer dipole moment,” *Russian Journal of Physical*

- Chemistry A **88**, 1431–1435 (2014).
- [47] G. Maroulis, “Static hyperpolarizability of the water dimer and the interaction hyperpolarizability of two water molecules,” *J. Chem. Phys.* **113**, 1813–1820 (2000).
- [48] L. Angel and A. J. Stace, “Dissociation patterns of $(\text{H}_2\text{O})_n^+$ cluster ions, for $n=2\text{--}6$,” *Chem. Phys. Lett.* **345**, 277–281 (2001).
- [49] C. J. Hensley, J. Yang, and M. Centurion, “Imaging of isolated molecules with ultrafast electron pulses,” *Phys. Rev. Lett.* **109**, 133202 (2012).
- [50] T. Kierspel, C. Bomme, M. Di Fraia, J. Wiese, D. Aniel-ski, S. Bari, R. Boll, B. Erk, J. S. Kienitz, N. L. M. Müller, D. Rolles, J. Viefhaus, S. Trippel, and J. Küpper, “Photophysics of indole upon x-ray absorption,” *Phys. Chem. Chem. Phys.* **20**, 20205 (2018), arXiv:1802.02964 [physics].
- [51] J. K. Gregory, D. C. Clary, K. Liu, M. G. Brown, and R. J. Saykally, “The water dipole moment in water clusters,” *Science* **275**, 814–817 (1997).

Supplemental Material: Pure molecular beam of water dimer

Helen Bieker,^{1, 2, 3} Jolijn Onvlee,¹ Melby Johny,^{1, 2} Lanhai He,^{1, ||} Thomas Kierspel,^{1, 2, 3, §}
Sebastian Trippel,^{1, 2} Daniel A. Horke,^{1, 2, ‡} and Jochen Küpper^{1, 2, 3, *}

¹Center for Free-Electron Laser Science, Deutsches Elektronen-Synchrotron DESY, Notkestraße 85, 22607 Hamburg, Germany

²Department of Physics, Universität Hamburg, Luruper Chaussee 149, 22761 Hamburg, Germany

³Center for Ultrafast Imaging, Universität Hamburg, Luruper Chaussee 149, 22761 Hamburg, Germany

FRAGMENTATION CORRECTION OF MEASUREMENTS

The strong-field-ionization technique employed in this work can lead to fragmentation, such that clusters from the molecular beam contributed to smaller masses in the mass spectrum (MS). For example, the water monomer and water dimer signals at $m/q = 18$ u/e and 36 u/e, respectively, contained contributions due to fragmentation of larger water-clusters in the molecular beam. Therefore, measured intensities needed to be corrected for these fragmentation channels. In addition, background water inside the chamber was measured at 18 u/e and needed to be corrected for.

For the latter, background measurement were permanently performed during the experiments using the higher repetition rate of the laser compared to the valve. Laser pulses were arriving in the interaction region at the same time as the molecular beam and between two molecular beam pulses, such that for each data point a background measurement was performed. The background signal was subtracted from the measurements.

The fragmentation ratios of water dimer into smaller masses could be estimated and used for the calculation of the fraction of water dimer in the deflected and undeflected molecular beam [1]. In Fig. 1 the deflection profiles measured at masses corresponding to H^+ , O^+ and OH^+ are shown. In the region of 2.8 to 3.5 mm the deflection curves look identical to those for the water dimer, indicating that at these positions those are fragments from water dimer. The ratios of water dimer to H^+ , O^+ and OH^+ at a position of 3 mm are 0.3 , 0.8 , and 0.7 , respectively. For the calculation of the fraction of water dimer in the molecular beam for the undeflected beam, these ratios were used to estimate the amount of water dimer inside of the beam.

For larger clusters, only fragments were measured, such that the measured signal was not solely due to a specific cluster stoichiometry and the overall shape of the molecular beam profile arose from several larger water-clusters. All protonated-water-cluster ions recorded showed the same deflection behavior, see Fig. 2. An estimate of the exponential decay of the measured protonated water-clusters distribution showed that protonated water-clusters $n = 1 - 10$ contained 99.6 % of the overall intensity.

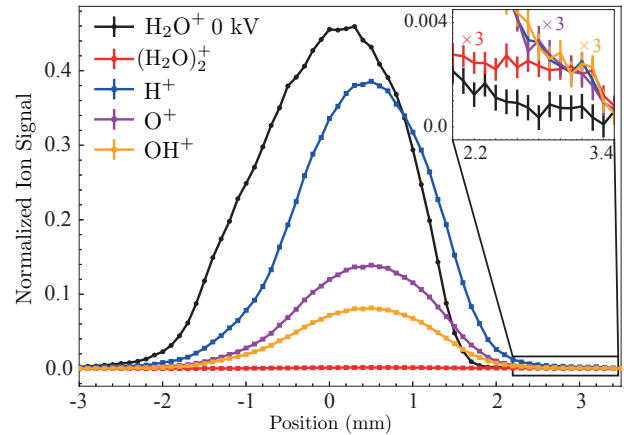


FIG. 1. Measured column density profiles of water with deflector voltages of 0 kV (black circles), H^+ , O^+ , OH^+ and water dimer with a deflector voltages of 8 kV (squares). The inset shows the region of 3 mm enlarged, where O^+ , OH^+ and the water dimer ion were scaled by 3 .

TRAJECTORY SIMULATIONS

The Stark energies and effective dipole moments μ_{eff} of water-clusters $n = 1 \dots 7$ were calculated using the freely available CMISTARK software package [2], which were then used to perform trajectory simulations [3] and to verify the measured deflection profiles of water-clusters. The rotational constants, dipole moments and centrifugal distortion constants from the literature are summarized in Table I. Three conformers for the water hexamer in prism-, book- and cage-like form [13] and two conformers of the water heptamer following the naming scheme of [15] were included.

For these simulations the water-clusters were assumed to be rigid rotors. Since the water dimer is known to be a floppy molecule with large amplitude motions [7, 16], the corresponding energy spectra and the description of the interaction of the states would significantly complicate further analysis. Using a rigid rotor assumption enables an easier and faster description and it has been shown previously that this model can be used to fit pure rotational transitions of the water dimer to experimental measurements [8].

For the rotational states $J = 0 \dots 2$ of water and water dimer the Stark energies and the corresponding μ_{eff} as a

molecule	dipole moment μ (D)			rotational constants (MHz)			Centrifugal Distortion constants (kHz)							
	μ_a	μ_b	μ_c	A	B	C	Δ_J	Δ_{JK}	Δ_K	d_J	d_K			
H_2O	0	-1.86	0	[4]	835840.29	435351.72	278138.70	[5]	3.759×10^4	-1.729×10^5	9.733×10^5	1.521×10^4	4.105×10^4	[5]
H_2O_2	2.63	0	0	[6]	190327.0	6162.76	6133.74	[7]	0.044	4010	0	0	0	[8]
H_2O_3	0	0	0	[9]	6646.91	6646.91	0	[10]	—	—	—	—	—	
H_2O_4	0	0	0	[9]	3149.00	3149.00	1622.00	[11]	—	—	—	—	—	
H_2O_5	0.93	0	0	[9]	1859.00	1818.00	940.00	[12]	—	—	—	—	—	
H_2O_6 book	0.17	2.46	0.16	[13]	1879.47	1063.98	775.06	[13]	—	—	—	—	—	
H_2O_6 cage	1.63	0.32	1.13	[13]	2163.61	1131.2	1068.80	[14]	—	—	—	—	—	
H_2O_6 prism	2.41	0.88	0.42	[13]	1658.22	1362.00	1313.12	[13]	—	—	—	—	—	
H_2O_7 1	1.0	1.0	0.0	[15]	1304.44	937.88	919.52	[15]	0.457	-0.342	0.842	0.0377	0.63	[15]
H_2O_7 2	1.0	0.0	1.0	[15]	1345.16	976.88	854.47	[15]	0.044	0.000	0.0000497	0	0	[15]

TABLE I. Dipole moments, rotational constants and centrifugal distortion constants of water-clusters used in the Stark-effect calculations

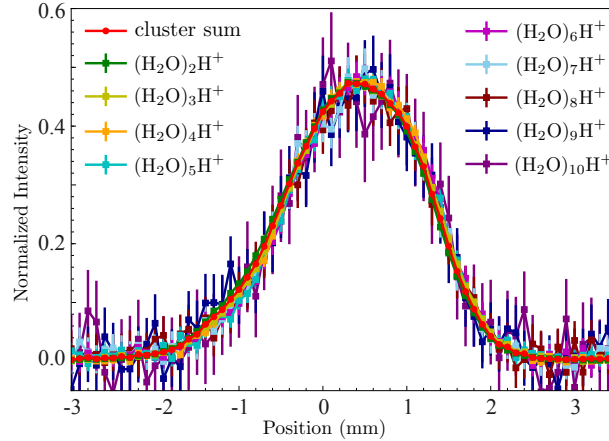


FIG. 2. Comparison of the averaged measured protonated-water-cluster signal (red) and the individual measured protonated-water-clusters deflection profiles for $n = 2 \dots 7$. The profiles are normalized to the area under the curve.

function of the electric field strength are shown in Fig. 3. For water dimer all relevant states are strong-field seeking and, hence, accelerated toward regions of stronger fields. For a nominal field strength of 50 kV/cm the μ_{eff} of the water dimer are significantly larger than for water monomer, except from the $|J, K_a, K_c, M\rangle = |2, 0, 2, 0\rangle, |2, 1, 1, 1\rangle$ states, leading to a larger acceleration in the electric field. All the shown states have a small asymmetry splitting, see Table I, resulting in a fast rise of μ_{eff} at small electric field strength. The discontinuous change of μ_{eff} at an electric field around 30 kV/cm is ascribed to an avoided crossing of the $|2, 2, 0, 2\rangle$ and $|3, 2, 2, 2\rangle$ states.

The trajectories of the molecules inside the electrostatic deflector were simulated using the calculated μ_{eff} [3]. For quantum states $J = 0 \dots 10, 10^7$ trajectories were calculated for each set of J states and used to simulate the spatial profiles using a weighting factor based on the thermal distributions of the state for a given temperature. Those temperature-weighted simulated vertical molecular-beam profiles were scaled to the area under the curve of the corresponding experimental profile to compare the deflection profiles. The simulations include

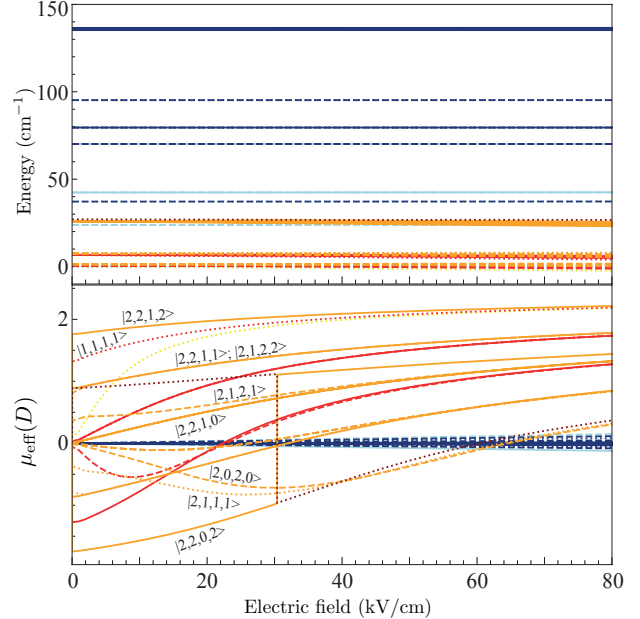


FIG. 3. Calculated Stark energy and effective dipole moments for the $J = 0 \dots 2$ states of water (blue) and water dimer (red, orange, yellow). $J = 0$ are shown in blue (water) and yellow (water dimer), $J = 1$ in light blue (water), red (water dimer), $J = 2$ in darkblue (water) and orange (water dimer) and the $|3, 2, 2, 2\rangle$ state in darkred for the water dimer. States where $K_a < K_c$ are indicated by dashed lines, $K_a > K_c$ by solid lines and $K_a = K_c$ by dotted lines.

the nuclear-spin-statistical weights for water and water dimer. For *para* and *ortho* water a room-temperature distribution of 1 : 3 was used. Water dimer in its equilibrium geometry is isomorphic with the permutation-inversion point group D_{4h} including tunneling splittings [17]. Neglecting tunneling splittings and acceptor switching, the rigid water dimer belongs to the symmetry group $C_S(M)$, yielding nuclear-spin-statistical weights of *para*:*ortho* of 16 : 16 [18].

The simulated profiles for water dimer at different rotational temperatures T_{rot} including rotational states $J = 0 \dots 10$ are shown in Fig. 4. An initial-beam temperature

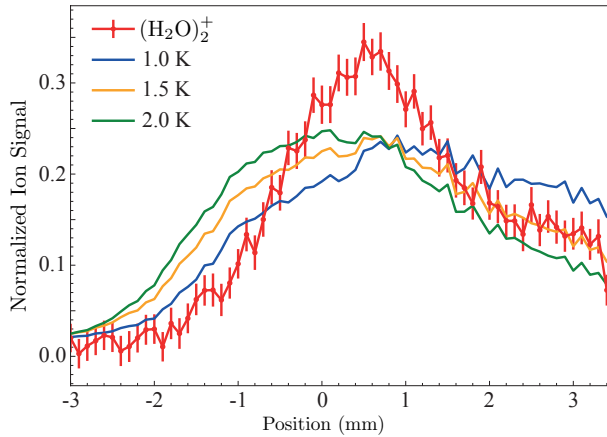


FIG. 4. Simulated deflection profiles for water dimer at temperatures of 1.0 K, 1.5 K and 2 K compared to the corrected pure water dimer profile at 8 kV (red, dots).

of $T_{\text{rot}} = 1.5(5)$ K reproduced the experiment the best. At this temperature water in the para nuclear spin state has 100 % of its population in its absolute rotational ground states $|J = 0, K_a = 0, K_c = 0, M = 0\rangle$, while ortho-water populates the $|J = 1, K_a = 0, K_c = 1, M = 0, 1\rangle$ state to equal amounts. 99.9 % of the para-water dimer and 99.9 % of the ortho-water dimer population is within $J = 0 \dots 10$.

Trajectory simulations were performed for water-clusters up to $n = 7$. Based on the estimated water-cluster distribution, *vide supra*, this covers 97.8 % of the water-clusters in the molecular beam, while ~ 2.2 % of the molecules in the beam are from water-clusters $n \geq 8$. The simulations for water-clusters including $J = 0 \dots 2$ and using the same rotational temperature $T_{\text{rot}} = 1.5(5)$ K of water dimer are shown in Fig. 5. We note that at

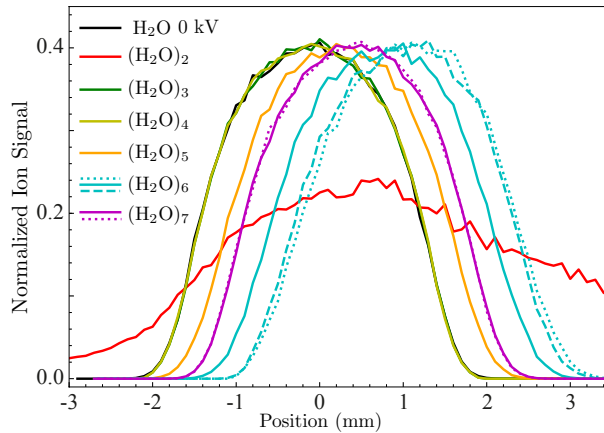


FIG. 5. Simulated deflection profiles for water-clusters for $n = 2 \dots 7$ are shown. Three different conformers of the water hexamer and two of water heptamer were included, see text for details.

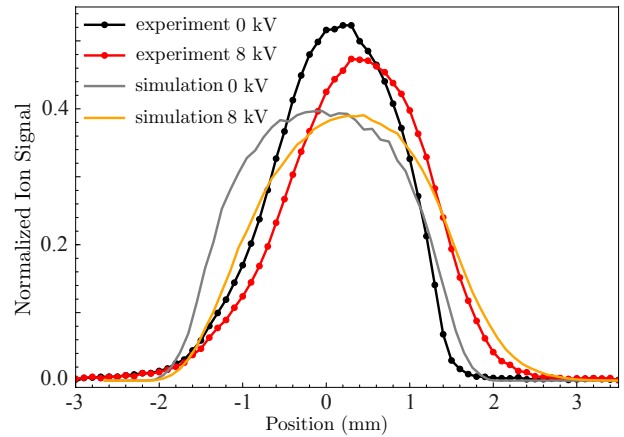


FIG. 6. Summed up simulated deflection profiles for water-clusters for $n = 3 \dots 7$ (grey, orange) and summed up measured deflection profiles for protonated water-clusters for $n = 2 \dots 10$ (black and red dots) for a deflector voltage of 0 kV (grey, black) and 8 kV (orange, red). The profiles are normalized to the area under the curve.

this temperature rotational states up to $J = 10$ might be populated in the molecular beam and the rotational temperature can differ from the one of water dimer. Thus the simulations give just an estimate of the amount of deflection. Based on the simulations the water dimer is deflecting the most of all water-clusters, followed by the water hexamer in prism- and book-like form, which reaches to a position of +3.2 mm.

Since for larger clusters only fragments have been measured and, therefore, the shape of the recorded beam profiles is the result of a superposition of several neutral cluster distributions in the molecular beam, it is not possible to compare the single deflection profiles directly with simulations. Therefore, at each position of the deflection profile the signal of the measured protonated water-clusters for $n = 2 \dots 10$ have been summed up. The H₃O⁺, $n = 1$, contained also signal from water dimer and has not been included. For the computationally derived profiles $n = 3 \dots 7$ were summed up for each position. As for the hexamer and heptamer several conformers have been simulated, each profile of the hexamer has been divided by 3 and for the heptamer by 2. This is shown in Fig. 6. These simulations assume a rather low temperature of 1.5 K and did not include the needed nuclear spin statistical weighting for larger-clusters. In addition, the decaying water-cluster distribution in the molecular beam was not taken into account, resulting in a slightly different deflection profile than the measured one. However, comparing the simulated and the measured deflection profiles, the deflection is on the same order of magnitude and the right-hand side tail of the simulated deflection profile is reaching up to a position of +3.2 mm.

-
- || Permanent address: Institute of Atomic and Molecular Physics, Jilin University, Changchun 130012, China
- § Present address: Department of Chemistry, University of Basel, Klingelbergstrasse 80, 4056 Basel, Switzerland
- ‡ Present address: Institute for Molecules and Materials, Radboud University, Heijendaalseweg 135, 6525 AJ Nijmegen, The Netherlands
- * Corresponding author: jochen.kuepper@cfel.de; <https://www.controlled-molecule-imaging.org>
- [1] M. Johny, J. Onvlee, T. Kierspel, H. Bieker, S. Trippel, and J. Küpper, “Spatial separation of pyrrole and pyrrole-water clusters,” *Chem. Phys. Lett.* **721**, 149–152 (2019), arXiv:1901.05267 [physics].
- [2] Y.-P. Chang, F. Filsinger, B. Sartakov, and J. Küpper, “CMISTARK: Python package for the stark-effect calculation and symmetry classification of linear, symmetric and asymmetric top wavefunctions in dc electric fields,” *Comp. Phys. Comm.* **185**, 339–349 (2014), arXiv:1308.4076 [physics].
- [3] F. Filsinger, J. Küpper, G. Meijer, L. Holmegaard, J. H. Nielsen, I. Nevo, J. L. Hansen, and H. Stapelfeldt, “Quantum-state selection, alignment, and orientation of large molecules using static electric and laser fields,” *J. Chem. Phys.* **131**, 064309 (2009), arXiv:0903.5413 [physics].
- [4] S. L. Shostak, W. L. Ebenstein, and J. S. Muenter, “The dipole moment of water. I. dipole moments and hyperfine properties of H₂O and HDO in the ground and excited vibrational states,” *J. Chem. Phys.* **94**, 5875 (1991).
- [5] F. C. DeLucia, P. Helminger, and W. H. Kirchhoff, “Microwave spectra of molecules of astrophysical interest V. Water vapor,” *J. Phys. Chem. Ref. Data* **3**, 211–219 (1974).
- [6] N. P. Malomuzh, V. N. Makhlaichuk, and S. V. Khrapatyi, “Water dimer dipole moment,” *Russian Journal of Physical Chemistry A* **88**, 1431–1435 (2014).
- [7] L. H. Coudert and J. T. Hougen, “Analysis of the microwave and far infrared spectrum of the water dimer,” *Journal Of Molecular Spectroscopy* **139**, 259–277 (1990).
- [8] T. R. Dyke, K. M. Mack, and J. S. Muenter, “The structure of water dimer from molecular beam electric resonance spectroscopy,” *J. Chem. Phys.* **66**, 498–510 (1977).
- [9] J. K. Gregory, D. C. Clary, K. Liu, M. G. Brown, and R. J. Saykally, “The water dipole moment in water clusters,” *Science* **275**, 814–817 (1997).
- [10] F. N. Keutsch, J. D. Cruzan, and R. J. Saykally, “The Water Trimer,” *Chemical Reviews* **103**, 2533–2578 (2003).
- [11] J. D. Cruzan, L. B. Braly, K. Liu, M. G. Brown, J. G. Loeser, and R. J. Saykally, “Quantifying hydrogen bond cooperativity in water: Vrt spectroscopy of the water tetramer,” *Science* **271**, 59–62 (1996).
- [12] K. Liu, M. G. Brown, J. D. Cruzan, and R. J. Saykally, “Vibration-rotation tunneling spectra of the water pentamer: Structure and dynamics,” *Science* **271**, 62–64 (1996).
- [13] C. Pérez, M. T. Muckle, D. P. Zaleski, N. A. Seifert, B. Temelso, G. C. Shields, Z. Kisiel, and B. H. Pate, “Structures of cage, prism, and book isomers of water hexamer from broadband rotational spectroscopy,” *Science* **336**, 897–901 (2012).
- [14] K. Liu, M. G. Brown, C. Carter, R. J. Saykally, J. K. Gregory, and D. C. Clary, “Characterization of a cage form of the water hexamer,” *Nature* **381**, 501–503 (1996).
- [15] C. Pérez, S. Lobsiger, N. A. Seifert, D. P. Zaleski, B. Temelso, G. C. Shields, Z. Kisiel, and B. H. Pate, “Broadband fourier transform rotational spectroscopy for structure determination: The water heptamer,” *Chemical Physics Letters* **571**, 1 – 15 (2013).
- [16] J. A. Odutola and T. R. Dyke, “Partially deuterated water dimers: Microwave spectra and structure,” *J. Chem. Phys.* **72**, 5062–5070 (1980).
- [17] T. R. Dyke, “Group theoretical classification of the tunneling-rotational energy levels of water dimer,” *J. Chem. Phys.* **66**, 492–497 (1977).
- [18] P. R. Bunker and P. Jensen, *Fundamentals of Molecular Symmetry*, Series in Chemical Physics (Institute of Physics Publishing, Bristol, UK, 2005).